Hydrogel-based reinforcement of 3D bioprinted constructs

2016 Biofabrication 8 035004

(http://iopscience.iop.org/1758-5090/8/3/035004)

Biofabrication

PAPER

Hydrogel-based reinforcement of 3D bioprinted constructs

RECEIVED
6 February 2016

REVISED
10 May 2016

ACCEPTED FOR PUBLICATION
23 June 2016

PUBLISHED
18 July 2016

Ferry P W Melchels[1,4,5], Maarten M Blokzijl[1,2,5], Riccardo Levato[1], Quentin C Peiffer[1], Mylène de Ruijter[1], Wim E Hennink[2], Tina Vermonden[2] and Jos Malda[1,3]

[1] Department of Orthopaedics, University Medical Center Utrecht, PO Box 85500, 3508 GA Utrecht, The Netherlands
[2] Department of Pharmaceutics, Utrecht Institute for Pharmaceutical Sciences (UIPS), Faculty of Science, Utrecht University, PO Box 80082, 3508 TB Utrecht, The Netherlands
[3] Department of Equine Sciences, Faculty of Veterinary Medicine, Utrecht University, PO Box 80163, 3508 TD Utrecht, The Netherlands
[4] Present address: Institute of Biological Chemistry, Biophysics and Bioengineering, School of Engineering and Physical Sciences, Heriot-Watt University, Edinburgh EH14 4AS, UK.
[5] These authors contributed equally to this work.

E-mail: j.malda@umcutrecht.nl

Keywords: bioprinting, tissue engineering, hydrogel, bioink, mechanical properties

Supplementary material for this article is available online

Abstract

Progress within the field of biofabrication is hindered by a lack of suitable hydrogel formulations. Here, we present a novel approach based on a hybrid printing technique to create cellularized 3D printed constructs. The hybrid bioprinting strategy combines a reinforcing gel for mechanical support with a bioink to provide a cytocompatible environment. In comparison with thermoplastics such as ϵ-polycaprolactone, the hydrogel-based reinforcing gel platform enables printing at cell-friendly temperatures, targets the bioprinting of softer tissues and allows for improved control over degradation kinetics. We prepared amphiphilic macromonomers based on poloxamer that form hydrolysable, covalently cross-linked polymer networks. Dissolved at a concentration of 28.6%w/w in water, it functions as reinforcing gel, while a 5%w/w gelatin-methacryloyl based gel is utilized as bioink. This strategy allows for the creation of complex structures, where the bioink provides a cytocompatible environment for encapsulated cells. Cell viability of equine chondrocytes encapsulated within printed constructs remained largely unaffected by the printing process. The versatility of the system is further demonstrated by the ability to tune the stiffness of printed constructs between 138 and 263 kPa, as well as to tailor the degradation kinetics of the reinforcing gel from several weeks up to more than a year.

1. Introduction

In recent years, 3D bioprinting has emerged as a technology platform showing potential for initiating drastic advances in drug testing, disease models, tissue engineering and regenerative medicine [1]. Bioprinting often employs hydrogels, in this context termed bioinks, in combination with cells to produce complex shapes using 3D printing technologies [2]. Three-dimensional cell culture generally requires hydrogels having low polymer concentrations, low stiffness and low cross-linking densities, to allow unhindered solute diffusion, cell migration and proliferation, as well as deposition of newly formed extracellular matrix [3, 4]. On the other hand, hydrogels for 3D printing with high shape fidelity ideally have high viscosity and yield stress to allow for spatially accurate extrusion, as well as rapid gelation and sufficient mechanical stability to maintain the shape of the final (cross-linked) gel [5].

Particularly for *in vivo* applications, mechanical stability is of utmost importance, and many of the employed bioinks lack sufficient mechanical properties [2]. One promising approach to overcome this hurdle is hybrid printing, in which the functions of mechanical support and cell encapsulation are separated into two materials. Most commonly, a bioink containing cells is co-printed with thermoplastics (ϵ-polycaprolactone in particular) [6–11], or UV curing adhesive [12]. While effective in improving mechanical properties, these materials either need high temperatures for processing, and/or show poor interaction between hydrophilic and hydrophobic

components. Furthermore, they allow limited control over the resulting mechanical properties, and importantly, over degradation kinetics. Particularly for the engineering of mechanically stable soft tissues, no ideal reinforcing material is currently available.

Here, we demonstrate a novel approach for the fabrication of mechanically stable biofabricated constructs, while maintaining control over degradation kinetics and mechanical properties. We aim to achieve this by separating the reinforcing and cell encapsulation functionalities into two distinct hydrogels: one with a high synthetic polymer concentration possessing excellent shape stability upon printing and one with a low natural polymer concentration exhibiting excellent cell encapsulation properties.

2. Materials and methods

2.1. Materials

Poloxamer 407 triblock copolymer (length of the PEG segments equal to 91 repeating units and the PPG segment is 56 units long (NMR)) was acquired from BASF (Ludwigshafen, Germany). D,L-lactide, glycolide and L-lactide were purchased from Corbion Purac (Gorinchem, The Netherlands). Irgacure 2959 was obtained from Ciba Specialty Chemicals (Basel, Switzerland). Solvents, unless indicated otherwise, were acquired from Biosolve (Valkenswaard, The Netherlands). Calcein acetoxymethyl ester (calcein-AM), Alamar Blue Cell viability reagent, Dulbecco's Modified Eagle's Medium (DMEM), penicillin, streptomycin and ethidium homodimer were acquired from Fisher Scientific (Landsmeer, The Netherlands). Deuterated chloroform ($CDCl_3$), ϵ-caprolactone, fluorescein isothiocyanate (FITC), gelatin (type A from porcine skin, 175 g bloom), methacrylic anhydride, sodium azide, stannous octoate ($Sn(Oct)_2$) and triethylamine (TEA) were all provided by Sigma Aldrich (Zwijndrecht, The Netherlands). Dialysis membranes (Spectra/Por 2, upper molecular weight cutoff 12–14 kDa) were obtained from Carl Roth (Karlsruhe, Germany). Cartridges and extrusion nozzles for 3D printing were obtained from Nordson EFD (Maastricht, The Netherlands). Biopsy punches were acquired from Milltex (Zaventem, Belgium).

All percentages concerning solutions are presented as %w/w, unless stated otherwise.

2.2. Poloxamer macromers synthesis and characterization

Poloxamer 407 was first dried by azeotropic distillation with toluene using a Dean Stark apparatus and then chain-extended by ring opening polymerization of either ϵ-caprolactone, D,L-lactide, or an equimolar mixture of L-lactide and glycolide for 1–2 d at 130 °C–150 °C in the presence of $Sn(Oct)_2$ as a catalyst, under a nitrogen atmosphere. The resulting polymers, and poloxamer 407 itself, were then dissolved in dry dichloromethane at a concentration of 20% and their terminal hydroxyl groups were reacted with a 3 times excess of methacrylic anhydride in the presence of an amount of triethylamine equal to the amount of methacrylic anhydride added. During the reaction, samples were taken and their NMR spectra were recorded in $CDCl_3$. When insufficient conversion was observed, another 3 times excess methacrylic anhydride and an equimolar amount of triethylamine were added to the reaction mixture. Purification was realized by precipitation from diethyl ether and drying under ambient conditions. The resulting macromonomers (macromers) are abbreviated as P-CL-MA, P-LA-MA and P-LG-MA, with ϵ-caprolactone, D,L-lactide or L-lactide-*co*-glycolide oligoesters, respectively. The macromer not possessing any hydrolysable ester will be referred to as P-MA. The targeted block lengths for the terminal ester blocks were 1 repeating unit for caprolactone, 2 for D,L-lactide and a combined total of 4 for L-lactide-*co*-glycolide. Poloxamer macromers were analyzed using ^{1}H NMR (Varian 400 MHz), with samples dissolved in $CDCl_3$. More detailed information on macromer composition, analysis and acronyms is available in the supporting info.

2.3. Gelatin methacryloyl synthesis and characterization

GelMA was synthesized by reacting gelatin with methacrylic anhydride, as reported previously [13]. FITC-labeled gelMA was created by reacting FITC with gelMA in a 0.1 M $NaHCO_3$ buffer at a pH of 9. For purposes of illustration, FITC-labeled gelMA was then used to create images of samples where it would otherwise be difficult to discriminate between poloxamer gel and gelMA.

2.4. Rheological characterization

Reinforcing gels were prepared by dissolving modified and unmodified poloxamer 407 at 28.6% in PBS. Their flow behavior was analyzed using a DHR2 rheometer (TA Instruments, Etten-Leur, The Netherlands), equipped with a Peltier plate and 40 mm cone, having a cone angle of 2°, at a truncation gap of 54 μm. Viscosity as a function of temperature was measured by heating the plate from 4 to 25 °C at a rate of 5 °C min^{-1}. A shear rate of 100 s^{-1} was applied to approximate the shear rate experienced by gels in the nozzle of a 3D printer. Yield shear stress was measured by gradually increasing the torque from 0 to beyond the point where flow was observed. The stress value assigned to the yield stress was calculated by determining the peak value of the derivative of viscosity versus stress. Shear thinning behavior was measured by recording the viscosity as a function of shear rate from 0.003 to 1000 s^{-1} at a temperature of 21 °C.

2.5. Construction of reinforced 3D printed gels

The reinforcing gel was prepared by adding P-MA to PBS at a concentration of 28.6% and was subsequently dissolved over 36 hours at 4 °C. GelMA was dissolved at a concentration of 5% in PBS at 37 °C for one hour. Both gel-precursors were supplemented with 0.1% Irgacure 2959.

CAD-models of various anatomical objects were translated into g-code using MMconverter (regenHU, Villaz-St-Pierre, Switzerland), applying a layer height of 0.24 mm and a strand spacing of 1.8 mm. Strand spacing indicates the distance between the midpoints of adjacent strands in the horizontal plane. Alternatively, samples for the analysis of printed construct stiffness were created by manually drawing the printer path in vector graphics and translating this into g-code using BioCAD (regenHU, Villaz-St-Pierre, Switzerland). Layer height was set at 0.24 mm and a total height of 2.16 or 0.96 mm was used for samples for mechanical testing and cytocompatibility tests, respectively. In both cases, the produced g-code can be read and executed on a 3DDiscovery bioprinter (regenHU, Villaz-St-Pierre, Switzerland). The bioprinter was provided with two cartridges. One was filled with the reinforcing gel and the other filled with the bioink. Print cartridges were kept at room temperature and 37 °C, respectively. Extrusion was air-pressure driven and for the reinforcing gel its pressure was set at 1.2 bar and 0.5 bar for the gelMA gel. Conical nozzles (27G) were used for deposition of reinforcing gel, whereas gelMA gels were deposited using a temperature controlled microvalve and nozzle (regenHU, Villaz-St-Pierre, Switzerland), with an inner diameter of 0.3 mm. Each deposited layer was illuminated for 10 seconds using a built-in UV-led ($\lambda = 365$ nm, $E = 240.2$ mW cm^{-2} at $h = 1$ cm) and completely built samples were subjected to an additional 15 min post cross-linking using a Vilber Lourmat portable UV-lamp ($\lambda = 365$ nm, $E = 3$ mW cm^{-2} at $h = 2$ cm) (Hartenstein, Würzburg, Germany).

Different strand distances were used to create samples with varying weight ratios of P-MA reinforcing gel to gelMA bioink. The stiffness of these constructs was subsequently measured as described below in section 2.7.

2.6. Hydrolytic degradation of reinforcing gels

Macromers P-MA, P-CL-MA, P-LA-MA, P-LG-MA as well as a 1:1 mixture of P-LA-MA and P-CL-MA were dissolved in PBS at a concentration of 28.6% with 0.1% Irgacure 2959. Gel precursor solutions were obtained after 36 hours of dissolution at 4 °C, these were injected into molds and subsequently cross-linked using a UV cross-linker (CL-1000, $\lambda = 365$ nm, 10.9 mW cm^{-2} at $h = 6$ cm) (UVP, Cambridge, United Kingdom) for 15 min to yield disks with a diameter and height of 6 and 2 mm, respectively. To study degradation, gels were placed in 50 ml PBS supplemented with 0.02% sodium azide to prevent bacterial growth and stored at 37 °C.

2.7. Mechanical characterization

Printed gel squares were cut to similar size as the molded gels using a 6 mm diameter biopsy punch. Both printed and cast samples were then subjected to uniaxial, unconfined compression at a strain rate of 30% min^{-1} between two parallel plates using a Q800 dynamical mechanical analyzer (TA Instruments, Etten-Leur, The Netherlands), up to 20% strain. Stiffness of the printed samples and Youngs modulus of the cast gels was calculated from the slope of the stress–strain curve between 3% and 10% strain.

2.8. Cell viability

Equine chondrocytes were isolated from the metacarpal joint of a deceased healthy adult donor, age 5 years. Cells at passage 1 were suspended at a concentration of 1×10^6 cells ml^{-1} in a 5% gelMA solution with 0.1% Irgacure 2959 in PBS at 37 °C. This cell-containing bioink was then printed four layers high, with either 28.6% P-MA or P-LG-MA based hydrogels as reinforcing material and using similar settings as those used to obtain samples for tuning the stiffness.

Printed samples containing encapsulated cells were cultured for up to 14 days in DMEM supplemented with 10% fetal calf serum and 1% penicillin/streptomycin. Assessment of cell viability was performed at day 1, 7 and 14 using calcein-AM and ethidium homodimer to label living and dead cells, respectively. Samples were incubated for 15 min in Dulbecco PBS supplemented with 25 μM calcein-AM and 2 μM ethidium homodimer. From each sample three pictures were taken using an IX53 microscope with XC50 camera (Olympus, Zoeterwoude, The Netherlands) and cells labeled red or green were counted using ImageJ software.

Metabolic activity of cells encapsulated in printed constructs was evaluated using the Alamar Blue reagent at day 1, 3, 7 and 14. For analysis, samples were incubated for four hours with DMEM supplemented with 10% Alamar Blue. The supernatant media was collected and analyzed on a Fluoroskan Ascent FL microplate reader (Thermo Scientific, Breda, The Netherlands) using an excitation and detection wavelength of 570 nm and 590 nm, respectively. Fluorescence intensity was compared against a calibration curve composed of known chondrocyte numbers.

2.9. Statistical methods

Each experiment was performed in three to six replicates ($n = 3 - n = 6$). Data are presented as mean and standard deviation of the replicates. A student's t-test was applied assuming Gaussian distribution of the data and p-values lower than 0.05 were considered as significantly different.

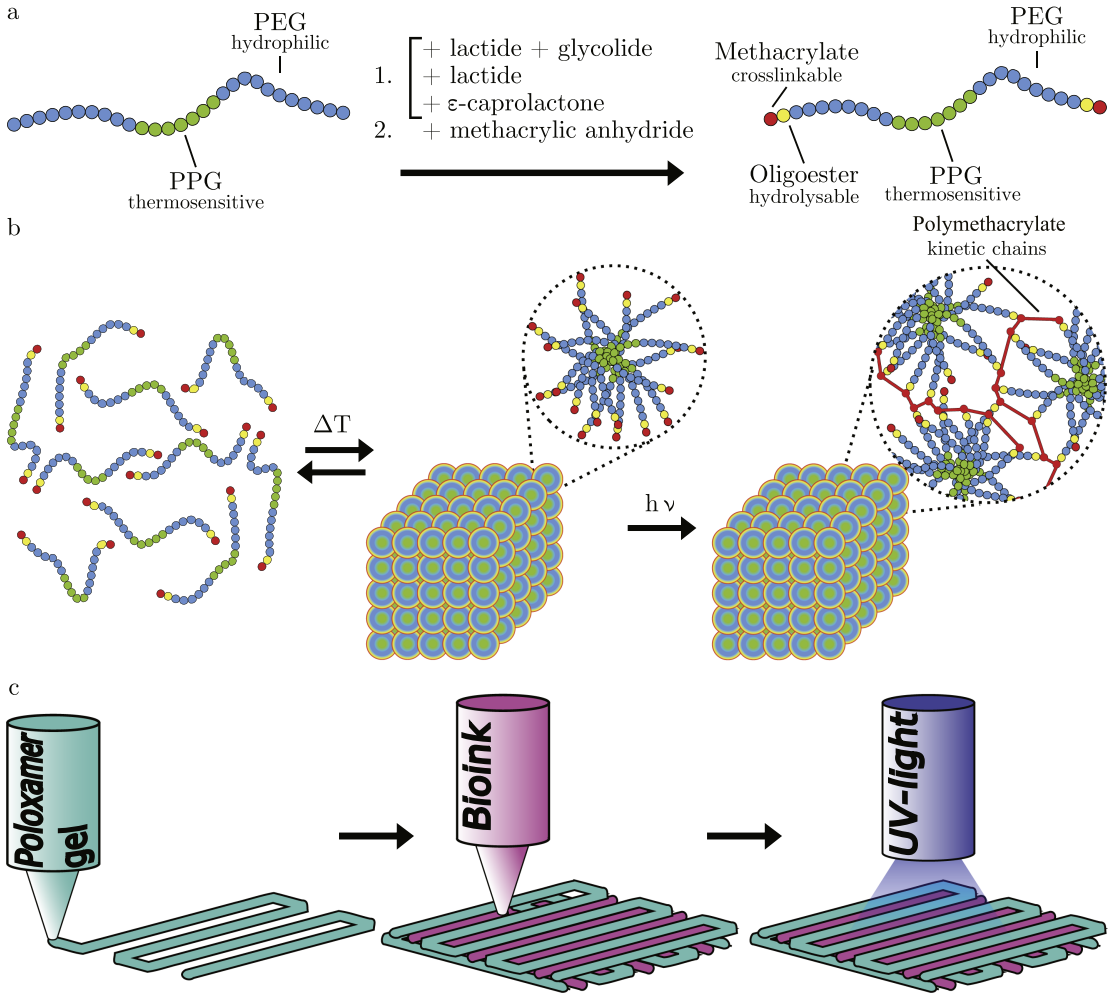

Figure 1. Schematic depictions of (a) the modification of poloxamer 407 with oligoesters and methacrylate moieties and (b) the temperature-dependent aggregation of modified poloxamer 407 in an aqueous environment. Also shown is the formation of polymethacrylate chains, linking individual macromers together. (c) Deposition strategy used to create reinforced gel constructs, with subsequent layers alternating between a 0°and 90°strand orientation.

3. Results and discussion

3.1. Poloxamer macromer synthesis and characterization

Building on previous work [14], we have developed printable hydrogels based on modified poloxamer 407. Poloxamer 407 was selected for modification because hydrogels based on poloxamer present excellent properties for 3D printing [14–16]. These triblock copolymers were chain-extended with α-hydroxy acids and methacrylate moieties, yielding three different hydrolysable macromonomers. Additionally, a non-degradable variant was also synthesized that does not possess an oligoester spacer. In aqueous environments, these macromers exhibit a lower critical solution temperature (LCST). At temperatures below the LCST, the PPG segments are hydrated, while at elevated temperatures they dehydrate and aggregate, resulting in the entropy-driven formation of micelles. Above the critical aggregation concentration (CAC) and LCST, the PEG coronas start to overlap and entangle, resulting in the formation of a highly viscous physical gel [17]. The process of chain extension and modification, as well as UV polymerization and printing strategy, is schematically shown in figure 1. Modified poloxamer 407 gels exhibit shear thinning behavior when the imposed shear stress exceeds the yield shear stress, as occurs in the nozzle of a 3D printer [13]. We selected a reinforcing gel concentration of 28.6% (0.4 g per ml solvent), which is above the CAC [17] and was found to be sufficient for 3D printing application, while yielding stiff gels with rubber-like appearance after cross-linking under ambient conditions.

3.2. Rheological characterization

The modified poloxamer-based hydrogels exhibit a nearly identical rheological behavior when compared to gels based on unmodified poloxamer. Two rheological phenomena critical to suitability for 3D printing are observed to a similar extent in all gels, being shear thinning and yield stress, as shown in figures 2(a) and (b), respectively. The Herschel–Bulkley model, which combines these two properties of non-Newtonian fluid

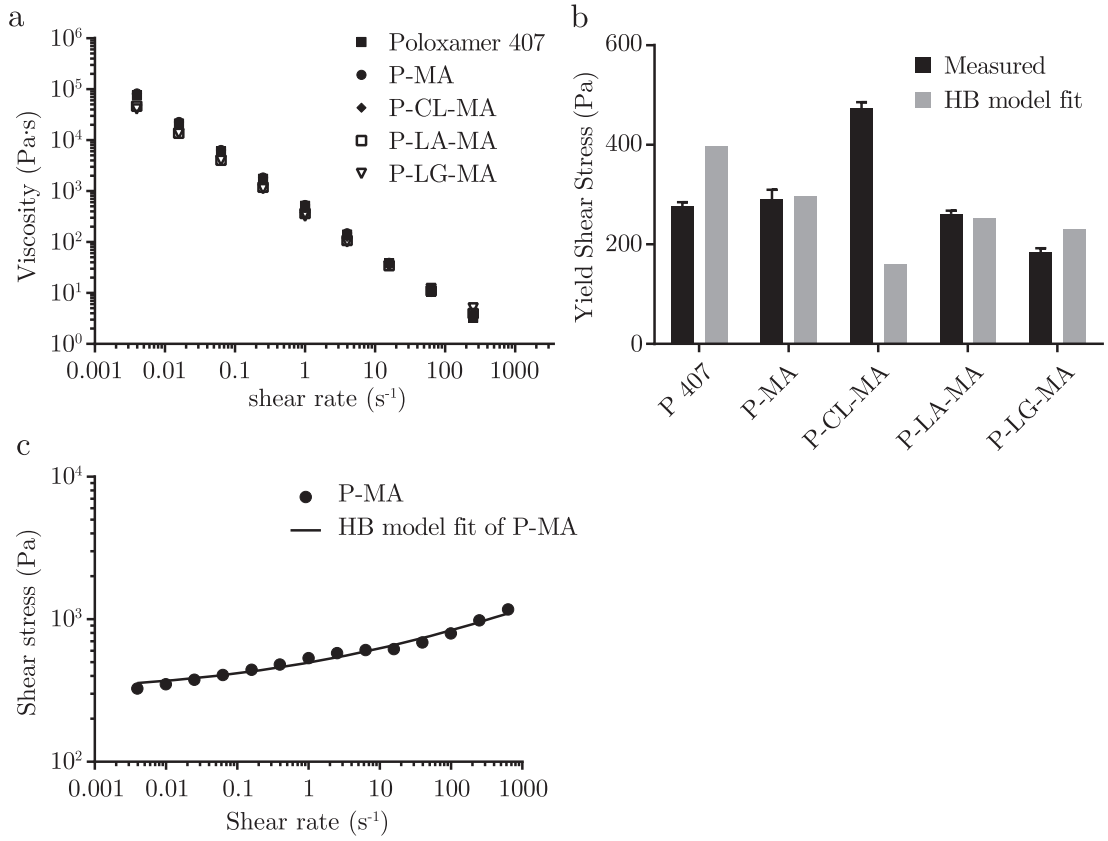

Figure 2. (a) Shear thinning behavior of reinforcing gels, (b) directly measured yield shear stress for the four reinforcing gels and unmodified poloxamer gel compared against extrapolated yield stress from the Herschel–Bulkley model and (c) fit of Herschel–Bulkley model to shear stress over rate data for P-MA based gels.

Table 1. Herschel–Bulkley fitting parameters applied to shear stress over rate data obtained from shear rate sweeps. With consistency index K and flow index n.

	K (Pa s)	n (—)	R^2
P 407	44.7	0.45	0.96
P-MA	199.2	0.22	0.98
P-CL-MA	315.2	0.11	0.92
P-LA-MA	66.6	0.47	0.99
P-LG-MA	83.0	0.46	0.99

behavior, was fitted to flow sweep data for all gels with high correlation as demonstrated in figure 2(c) and table 1. Values of n much smaller than unity confirm the shear thinning effect, while yield stresses of several hundred Pa are sufficient to prevent sagging of printed structures. The yield stress derived from the Herschel–Bulkley model represents residual stress that remains when extrapolating to zero shear rate. Therefore, its value is sensitive to the range of data points selected for fitting; for all gels we used 28 data points in the same range ($4{\cdot}10^{-3}$–1000 s^{-1}), at logarithmic intervals.

In addition, we directly measured yield stress for each gel by slowly increasing torque on a static gel in the rheometer. The yield point is defined as the first point at which a strain can be measured. This indicates initiation of flow, and it is followed by a large drop in viscosity upon further increase in torque. Directly measured yield stress is highly reproducible, with values being in the same order of magnitude as fitted values (figure 2(b)).

The higher yield stress observed for P-CL-MA based gels could originate from the higher hydrophobicity of caprolactone, thus exhibiting a stronger interaction with the hydrophobic PPG domains when compared to the three other macromers, which are slightly more hydrophilic. This effect has actually been exploited to achieve more stable poloxamer-based micelles previously [18].

Temperature sweeps (figure S2 in supplementary information) showed 1°C–5°C shifts upwards for the LCST value of modified poloxamers as compared to unmodified poloxamer (LCST = 12 °C). Although the thermosensitivity is not directly exploited in the ambient printing process (other than facilitating loading of cartridges using cold solutions), it further confirms that the oligoester and methacrylate modification has had limited effect on the rheological behavior of highly printable poloxamer 407 based hydrogels.

3.3. Construction of reinforced 3D printed gels

As can be seen from figure 3, the hybrid 3D bioprinting approach proposed allows for the generation of complex shapes. Here, the reinforcing gel strands were found to be 0.3 mm wide. The selected bioink was

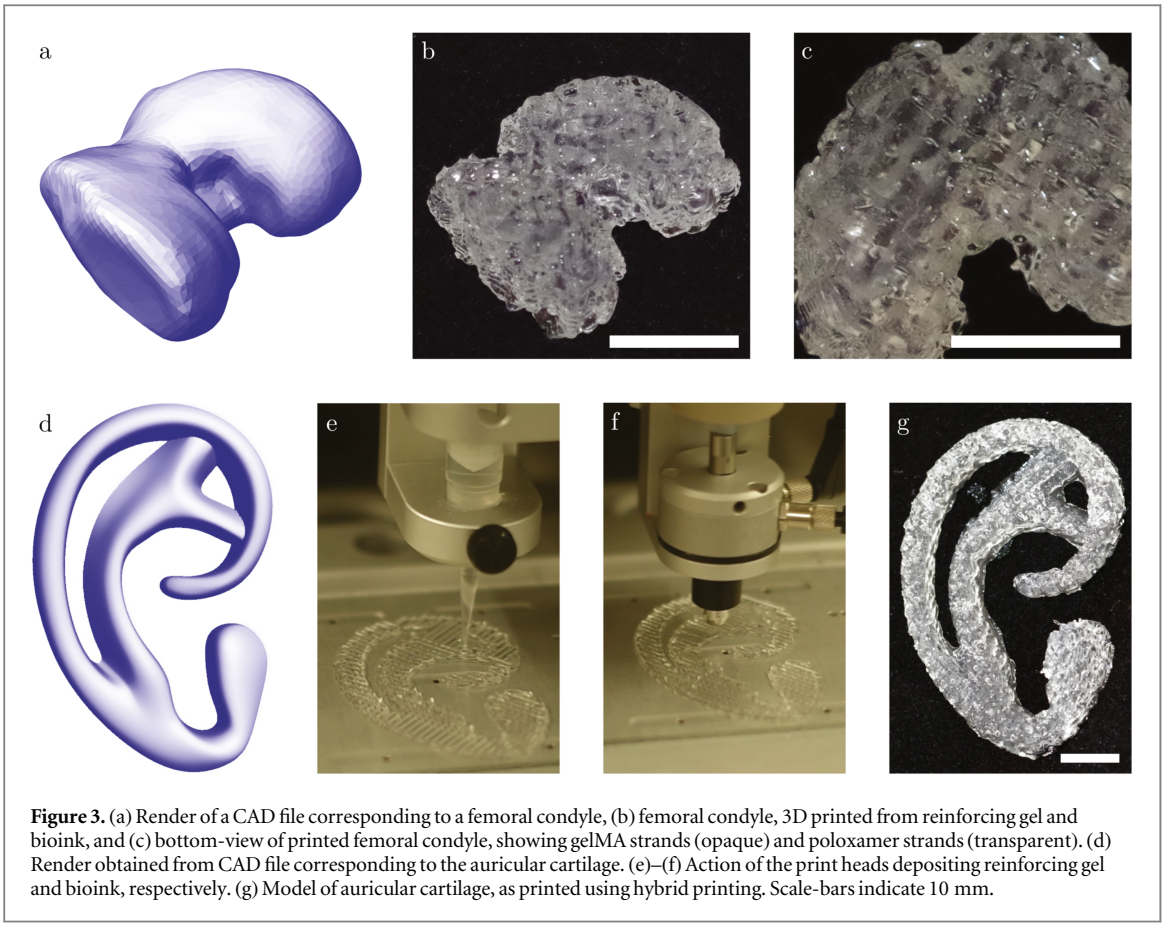

Figure 3. (a) Render of a CAD file corresponding to a femoral condyle, (b) femoral condyle, 3D printed from reinforcing gel and bioink, and (c) bottom-view of printed femoral condyle, showing gelMA strands (opaque) and poloxamer strands (transparent). (d) Render obtained from CAD file corresponding to the auricular cartilage. (e)–(f) Action of the print heads depositing reinforcing gel and bioink, respectively. (g) Model of auricular cartilage, as printed using hybrid printing. Scale-bars indicate 10 mm.

composed of 5% gelatin methacryloyl (gelMA), for its desirable properties for cell encapsulation [19–22]. Previously, 3D printing of bioinks based on 10% gelMA was realized by addition of viscosity or gelation modifiers [13, 23], or by strictly controlling temperature [20]. Here, a gelMA bioink with a concentration as low as 5% was deposited in-between strands of P-MA reinforcing gel, building a 3D construct up 10 mm high. To demonstrate the improved control over printed geometry, also a more challenging shape was produced, resembling the auricular cartilage.

This hybrid bioprinting approach allows control over the mechanical properties of the construct within a specific range, by altering the composition of the 3D print. Specifically, this can be achieved by increasing or decreasing the distance between adjacent strands of the reinforcing gel, thus influencing the weight ratio of reinforcing gel with respect to the bioink in the printed construct. This approach resulted in the ability to tailor the overall stiffness of printed gel constructs. For instance, a strand spacing of 2.7 mm yielded a stiffness of 138 $\pm$ 25 kPa, while decreasing this distance to 1.35 mm increased the overall stiffness about two fold to 263 $\pm$ 48 kPa, as can be seen from figure 4. The achieved stiffness demonstrated here is considerably lower than that of samples reinforced using thermoplastics such as polycaprolactone, which exhibit stiffness values up to several MPa [9, 24]. For this reason, reinforcing gels may be particularly advantageous for the bioprinting of soft tissues, for which currently very few options for reinforcing exist.

3.4. Cell viability and metabolic activity

To demonstrate the cytocompatibility of this hybrid bioprinting approach, equine chondrocytes embedded within a 5% gelMA gel were co-printed with P-MA or P-LG-MA reinforcing gel into a hybrid construct. When compared to cells encapsulated in the cast gelMA control, viability did only differ significantly on the first day after printing, as represented in figure 5(a). On days 7 and 14 viability was similar for all three groups and passed the 90% mark on day 14. Cell viability after two weeks remains largely unaffected by the hybrid printing approach.

On the other hand, metabolic activity, as shown in figure 5(b) shows a more pronounced difference between the three groups, especially at day 14. Even so, it should be noted that an increase of metabolic activity may be observed over time. Lower metabolic activity found for hybrid scaffolds using P-LG-MA based reinforcing gels could be explained by a loss of structural integrity due to rapid degradation of the reinforcing component. Our data suggests that cells inside the gelMA component of the hybrid printed scaffolds survive and proliferate. Even though free poloxamer above a critical concentration could be harmful to cells [25], it

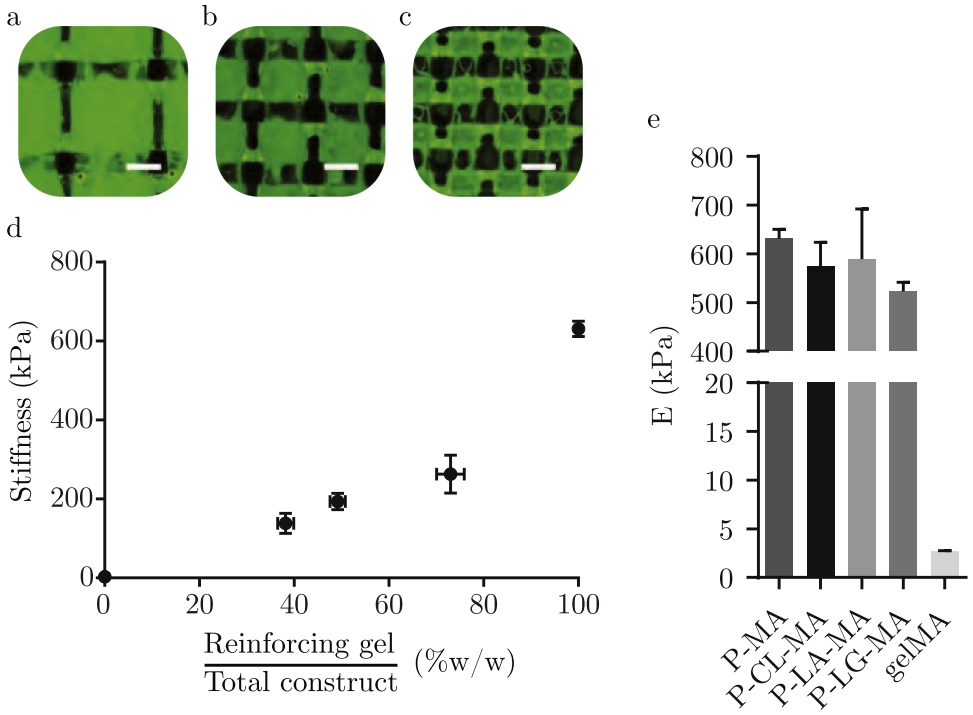

Figure 4. (a)–(c) Fluorescence microscopy pictures corresponding to hybrid printed structures with strand distances of 2.7, 1.8 and 1.35 mm, respectively. GelMA appears green, whereas P-MA reinforcing gel is unstained and appears dark. Scale bars indicate 1 mm. (d) Stiffness as a function of the weight percentage of reinforcing gel deposited to create hybrid 3D printed structures. A strand spacing of 2.7, 1.8 and 1.35 mm was used to produce gels with a weight ratio of reinforcing gel of 38.2 ± 1.7, 49.2 ± 1.6 and 73.0 ± 2.9 %w/w, respectively. The stiffness of cast 5% gelMA and 28.6% P-MA gel disks is included for comparison and for 5% gelMA, i.e. 0% reinforcing gel, this is equal to 2.7 kPa. (e) Comparison of stiffness of 28.6% P-MA, P-CL-MA, P-LA-MA, P-LG-MA and 5% gelMA gels.

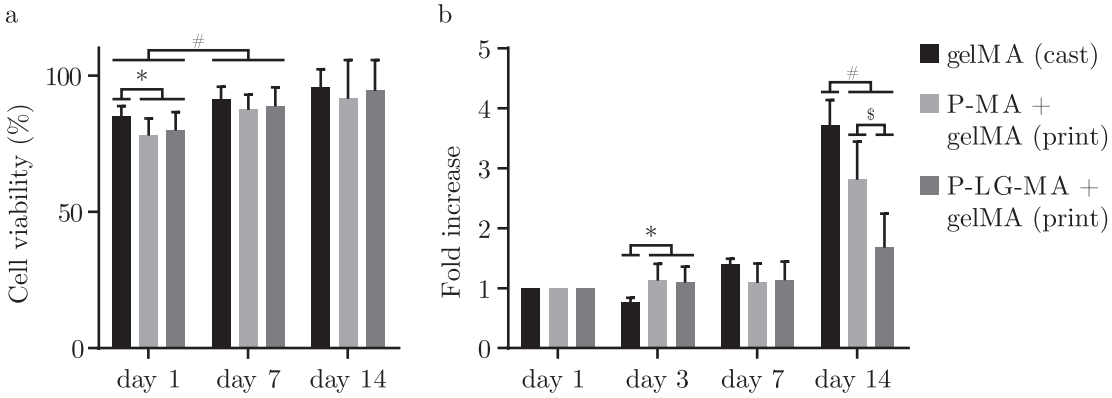

Figure 5. (a) Cell viability within the bioink of printed P-MA and P-LG-MA reinforced constructs at day 1, 7 and 14, compared to cell viability within cast gelMA gels. (b) Metabolic activity of equine chondrocytes within printed constructs, normalized to the activity on day 1 for each condition at day 1, 3, 7 and 14. *, #, $ are used to indicate $p < 0.05$.

is unlikely that these concentrations are achieved in culture using the hybrid printing approach in combination with fast degrading modified poloxamer-based gels.

3.5. Hydrolytic degradation of reinforcing gels

Regenerative approaches aim to fully restore the tissue which means that over time, the implanted material should be cleared from the body and its function taken over by newly formed tissue [26]. This requires precise control over the timing and mechanism of scaffold degradation. However, not all currently investigated printable biomaterials allow fine-tuning of their degradation kinetics. Because of the flexibility of the modified poloxamer macromer platform, a broad range of degradation rates could be realized. Based on a principle first demonstrated by Hubbell in 1993 for poly(ethylene glycol) based hydrogels, incorporation of a degradable oligoester spacer between poloxamer and methacrylate moiety allows degradation of cross-linked hydrogels obtained from these macromers to be tuned as desired [27]. Considering figure 6 it can be seen that upon incubation in PBS at 37 °C, gel disks

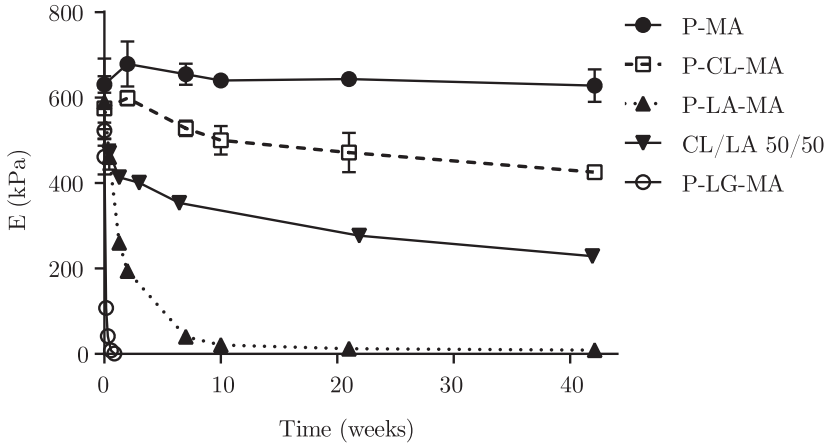

Figure 6. Youngs modulus of reinforcing gels after being submerged in PBS at 37 °C, measured over time. Also shown is a gel crosslinked from a 50/50 mixture of P-CL-MA and P-LA-MA macromers.

prepared from P-LG-MA macromers show a rapid decline in stiffness within the first week and fully dissociate within 2 weeks. On the contrary, P-CL-MA gels exhibit limited loss of structural integrity even after 40 weeks. Since poloxamer-oligoester based gels degrade via bulk degradation, mass loss of the hydrated gel is negligible up to the point where no covalent crosslinks remain. Beyond this point, gels disintegrate and dissolve rapidly [28]. All gels tested in this study, except those composed of P-MA, show a decline in Youngs modulus over time.

4. Conclusion

In order for a biofabrication strategy to be successful, it should fulfill both biological and mechanical aspects to an optimal extent. We have presented here a novel approach that can contribute towards the bioprinting of mechanically stable soft tissues, by separating these two functions into two different and specialized hydrogels. This has resulted in a strategy that allows for accurate control over mechanical properties and degradation kinetics. Finally, we would like to highlight the potential of this technique by mentioning it may also find application in other areas of research currently utilizing hydrogels, such as soft robotics [29], biosensors [30, 31] and artificial organs [1, 32], but foremost in tissue engineering, where it may contribute to the manufacturing of implantable, mechanically stable functional tissues.

Acknowledgments

We kindly acknowledge Iris Otto for providing us with a CAD model of the auricular cartilage. Research leading to this work has received funding from the Dutch Arthritis Foundation (LLP-12); the European Community's Seventh Framework Programme (FP7/2007-2013) under grant agreement 309962 (HydroZONES); and the European Research Council under grant agreement 647426 (3D-JOINT).

References

[1] Murphy S V and Atala A 2014 3D bioprinting of tissues and organs *Nat. Biotechnol.* **32** 773–85
[2] Malda J, Visser J, Melchels F P W, Jüngst T, Hennink W E, Dhert W J A, Groll J and Hutmacher D W 2013 25th Anniversary article: engineering hydrogels for biofabrication *Adv. Mater.* **25** 5011–28
[3] DeForest C A and Anseth K S 2012 Advances in bioactive hydrogels to probe and direct cell fate *Annu. Rev. Chem. Biomol. Eng.* **3** 421–44
[4] Seliktar D 2012 Designing cell-compatible hydrogels for biomedical applications *Science* **336** 1124–8
[5] Jungst T, Smolan W, Schacht K, Scheibel T and Groll J 2015 Strategies and molecular design criteria for 3D printable hydrogels *Chem. Rev.* **116** 1496–539
[6] Boere K W M, Visser J, Seyednejad H, Rahimian S, Gawlitta D, van Steenbergen M J, Dhert W J A, Hennink W E, Vermonden T and Malda J 2014 Covalent attachment of a three-dimensionally printed thermoplast to a gelatin hydrogel for mechanically enhanced cartilage constructs *Acta Biomater.* **10** 2602–11
[7] Pati F, Jang J, Ha D H, Kim S W, Rhie J W, Shim J H, Kim D H and Cho D W 2014 Printing three-dimensional tissue analogues with decellularized extracellular matrix bioink *Nat. Commun.* **5** 1–1
[8] Pati F, Ha D H, Jang J, Han H H, Rhie J W and Cho D W 2015 Biomimetic 3D tissue printing for soft tissue regeneration *Biomaterials* **62** 164–75
[9] Schuurman W, Khristov V, Pot M W, van Weeren P R, Dhert W J A and Malda J 2011 Bioprinting of hybrid tissue constructs with tailorable mechanical properties *Biofabrication* **3** 021001
[10] Shim J H, Kim J Y, Park M, Park J and Cho D W 2011 Development of a hybrid scaffold with synthetic biomaterials and hydrogel using solid freeform fabrication technology *Biofabrication* **3** 034102
[11] Visser J, Peters B, Burger T J, Boomstra J, Dhert W J A, Melchels F P W and Malda J 2013 Biofabrication of multi-material anatomically shaped tissue constructs *Biofabrication* **5** 035007
[12] Bakarich S E, Gorkin R, Spinks G M and in het Panhuis M 2014 Three-dimensional printing fiber reinforced hydrogel composites *ACS Appl. Mater. Interfaces* **6** 15998–6006
[13] Melchels F P W, Dhert W J A, Hutmacher D W and Malda J 2014 Development and characterisation of a new bioink for additive tissue manufacturing *J. Mater. Chem.* B **2** 2282

[14] Fedorovich N E, Swennen I, Girones J, Moroni L, van Blitterswijk C A, Schacht E, Alblas J and Dhert W J A 2009 Evaluation of photocrosslinked lutrol hydrogel for tissue printing applications *Biomacromolecules* **10** 1689–96
[15] Müller M, Becher J, Schnabelrauch M and Zenobi-Wong M 2015 Nanostructured pluronic hydrogels as bioinks for 3D bioprinting *Biofabrication* **7** 035006
[16] Kolesky D B, Truby R L, Gladman A S, Busbee T A, Homan K A and Lewis J A 2014 3D bioprinting of vascularized, heterogeneous cell-laden tissue constructs *Adv. Mater.* **26** 3124–30
[17] Lenaerts V, Triqueneaux C, Quartern M, Rieg-Falson F and Couvreur P 1987 Temperature-dependent rheological behavior of Pluronic F-127 aqueous solutions *Int. J. Pharmaceutics* **39** 121–7
[18] Zhang Y, Zhao L, Chen M and Lang M 2013 Synthesis and properties of Pluronic-based pentablock copolymers with pendant amino groups *Colloid Polym. Sci.* **291** 1563–71
[19] Aubin H, Nichol J W, Hutson C B, Bae H, Sieminski A L, Cropek D M, Akhyari P and Khademhosseini A 2010 Directed 3D cell alignment and elongation in microengineered hydrogels *Biomaterials* **31** 6941–51
[20] Billiet T, Gevaert E, De Schryver T, Cornelissen M and Dubruel P 2014 The 3D printing of gelatin methacrylamide cell-laden tissue-engineered constructs with high cell viability *Biomaterials* **35** 49–62
[21] Chen Y C, Lin R Z, Qi H, Yang Y, Bae H, M-Martin J M and Khademhosseini A 2012 Functional human vascular network generated in photocrosslinkable gelatin methacrylate hydrogels *Adv. Funct. Mater.* **22** 2027–39
[22] Nichol J W, Koshy S T, Bae H, Hwang C M, Yamanlar S and Khademhosseini A 2010 Cell-laden microengineered gelatin methacrylate hydrogels *Biomaterials* **31** 5536–44
[23] Schuurman W, Levett P A, Pot M W, van Weeren P R, Dhert W J A, Hutmacher D W, Melchels F P W, Klein T J and Malda J 2013 Gelatin-methacrylamide hydrogels as potential biomaterials for fabrication of tissue-engineered cartilage constructs *Macromol. Biosci.* **13** 551–61
[24] Visser J, Melchels F P W, Jeon J E, van Bussel E M, Kimpton L S, Byrne H M, Dhert W J A, Dalton P D, Hutmacher D W and Malda J 2015 Reinforcement of hydrogels using three-dimensionally printed microfibres *Nat. Commun.* **6** 6933
[25] Khattak S F, Bhatia S R and Roberts S C 2005 Pluronic F127 as a cell encapsulation material: utilization of membrane-stabilizing agents *Tissue Eng.* **11** 974–83
[26] Hutmacher D W 2000 Scaffolds in tissue engineering bone and cartilage *Biomaterials* **21** 2529–43
[27] Sawhney A S, Pathak C P and Hubbell J A 1993 Bioerodible hydrogels based on photopolymerized poly(ethylene glycol)-co-poly(α-hydroxy acid) diacrylate macromers *Macromolecules* **26** 581–7
[28] Metters A T, Bowman C N and Anseth K S 2000 A statistical kinetic model for the bulk degradation of PLA-b-PEG-b-PLA hydrogel networks *J. Phys. Chem.* B **104** 7043–9
[29] Kim S, Laschi C and Trimmer B 2013 Soft robotics: a bioinspired evolution in robotics *Trends Biotechnol.* **31** 287–94
[30] Robinson S S, OBrien K W, Zhao H, Peele B N, Larson C M, Mac Murray B C, van Meerbeek I M, Dunham S N and Shepherd R F 2015 Integrated soft sensors and elastomeric actuators for tactile machines with kinesthetic sense *Extreme Mech. Lett.* **5** 47–53
[31] Sawahata K, Ping Gong J and Osada Y 1995 Soft and wet touch-sensing system made of hydrogel *Macromol. Rapid Commun.* **16** 713–6
[32] Melchels F P W, Domingos M A N, Klein T J, Malda J, Bartolo P J and Hutmacher D W 2012 Additive manufacturing of tissues and organs *Prog. Polym. Sci.* **37** 1079–104